Ratiometric spectral imaging for fast tumor detection and chemotherapy monitoring *in vivo*

Jae Youn Hwang
Zeev Gross
Harry B. Gray
Lali K. Medina-Kauwe
Daniel L. Farkas

Ratiometric spectral imaging for fast tumor detection and chemotherapy monitoring *in vivo*

Jae Youn Hwang,a,b,c Zeev Gross,d Harry B. Gray,e Lali K. Medina-Kauwe,c,f and Daniel L. Farkasa,b,c,g
aUniversity of Southern California, Department of Biomedical Engineering, Los Angeles, California 90089
bCedars-Sinai Medical Center, Minimally Invasive Surgical Technologies Institute and Department of Surgery,
Los Angeles, California 90048
cCedars-Sinai Medical Center, Department of Biomedical Sciences, Los Angeles, California 90048
dTechnion-Israel Institute of Technology, Schulich Faculty of Chemistry, Technion City, Haifa 32000, Israel
eCalifornia Institute of Technology, Beckman Institute, Pasadena, California 91125
fUniversity of California, David Geffen School of Medicine, Los Angeles, California 90095
gSpectral Molecular Imaging, Incorporated, Beverly Hills, California 90211

Abstract. We report a novel *in vivo* spectral imaging approach to cancer detection and chemotherapy assessment. We describe and characterize a ratiometric spectral imaging and analysis method and evaluate its performance for tumor detection and delineation by quantitatively monitoring the specific accumulation of targeted gallium corrole (HerGa) into HER2-positive (HER2+) breast tumors. HerGa temporal accumulation in nude mice bearing HER2+ breast tumors was monitored comparatively by a. this new ratiometric imaging and analysis method; b. established (reflectance and fluorescence) spectral imaging; c. more commonly used fluorescence intensity imaging. We also tested the feasibility of HerGa imaging *in vivo* using the ratiometric spectral imaging method for tumor detection and delineation. Our results show that the new method not only provides better quantitative information than typical spectral imaging, but also better specificity than standard fluorescence intensity imaging, thus allowing enhanced *in vivo* outlining of tumors and dynamic, quantitative monitoring of targeted chemotherapy agent accumulation into them. © *2011 Society of Photo-Optical Instrumentation Engineers (SPIE)*. [DOI: 10.1117/1.3589299]

Keywords: spectral imaging; chemotherapy; tumor detection; ratiometric; tumor-targeted gallium corrole.

Paper 10601RR received Dec. 14, 2010; revised manuscript received Apr. 10, 2011; accepted for publication Apr. 12, 2011; published online Jun. 9, 2011.

1 Introduction

Breast cancer is the most common cancer in women, and those diagnosed with HER2+ tumors suffer from a more aggressive type of breast cancer that is less responsive to standard interventions.[1] For decades, in order to reduce mortality, efforts have focused on new approaches for breast tumor treatment (especially chemotherapy) and its early detection.[2] We recently introduced optical imaging *in vivo* for chemotherapy assessment,[3] and reported that a tumor-targeted gallium corrole (HerGa), comprising sulfonated gallium corrole (S2Ga) complexed with the recombinant tumor-targeting cell penetrating protein, HerPBK10, is highly effective for killing HER2+ breast cancer cells *in vitro*[4] as well as for tumor detection and treatment in an animal model of HER2+ breast cancer.[5] In those studies, we used fluorescence intensity imaging to validate the tumor-targeting capability of HerGa *in vivo* and *ex vivo*. However, during the fluorescence intensity imaging of HerGa, the blue light used for its excitation also produced significant autofluorescence, and the penetration depths of the light were limited to a few millimeters. Furthermore, the nonhomogeneous *in vivo* accumulation of HerGa introduced artifacts. These limitations resulted in reduced contrast in the quantitative analysis for monitoring of preferential accumulation of HerGa and tumor detection *in vivo*.[5] For successful translation

of HerGa chemotherapy into the clinic, we need to improve the contrast and the accuracy in the imaging-based monitoring of HerGa for tumor detection. This challenge motivated an effort to develop new methods with improved quantification and specificity.

Spectral imaging has been widely utilized as a useful quantitative method in biomedical research such as functional imaging of brain oxygenation,[6] melanoma evaluation,[7] and determining the targeting capacity of molecules to specific tissues *in vivo*.[8] In typical spectral imaging, spectral signatures are generally analyzed by various classification techniques such as Euclidean distance, correlation, and spectral angle measurements, resulting in a classified image that can provide quantitative discrimination between signals from molecules of interest and unwanted signals, with high sensitivity and specificity.[9] However, when the molecules are administered intravenously (i.v.), standard spectral imaging and analysis may not be best suited to rapidly determine whether the molecules are preferentially accumulated into targeted tissues, since fast detection of these fluorophores at the locations of interest needs to occur over a significant background signal originating from the same molecules distributed nonspecifically (and over the whole mouse) through blood vessels, within a few minutes. Applying a straightforward spectral classification would therefore, under these circumstances, yield low specificity results, certainly until the nontargeted molecules are cleared from their body. Therefore, the implementation of these methods is hampered by inherent limitations.

Address all correspondence to: Daniel Farkas,Cedars-Sinai Medical Center, Davis 4021–8700 Beverly Boulevard, Los Angeles, California 90048. Tel: 310–423-7746; Fax: 310–423-7707; E-mail: dlfarkas@gmail.com
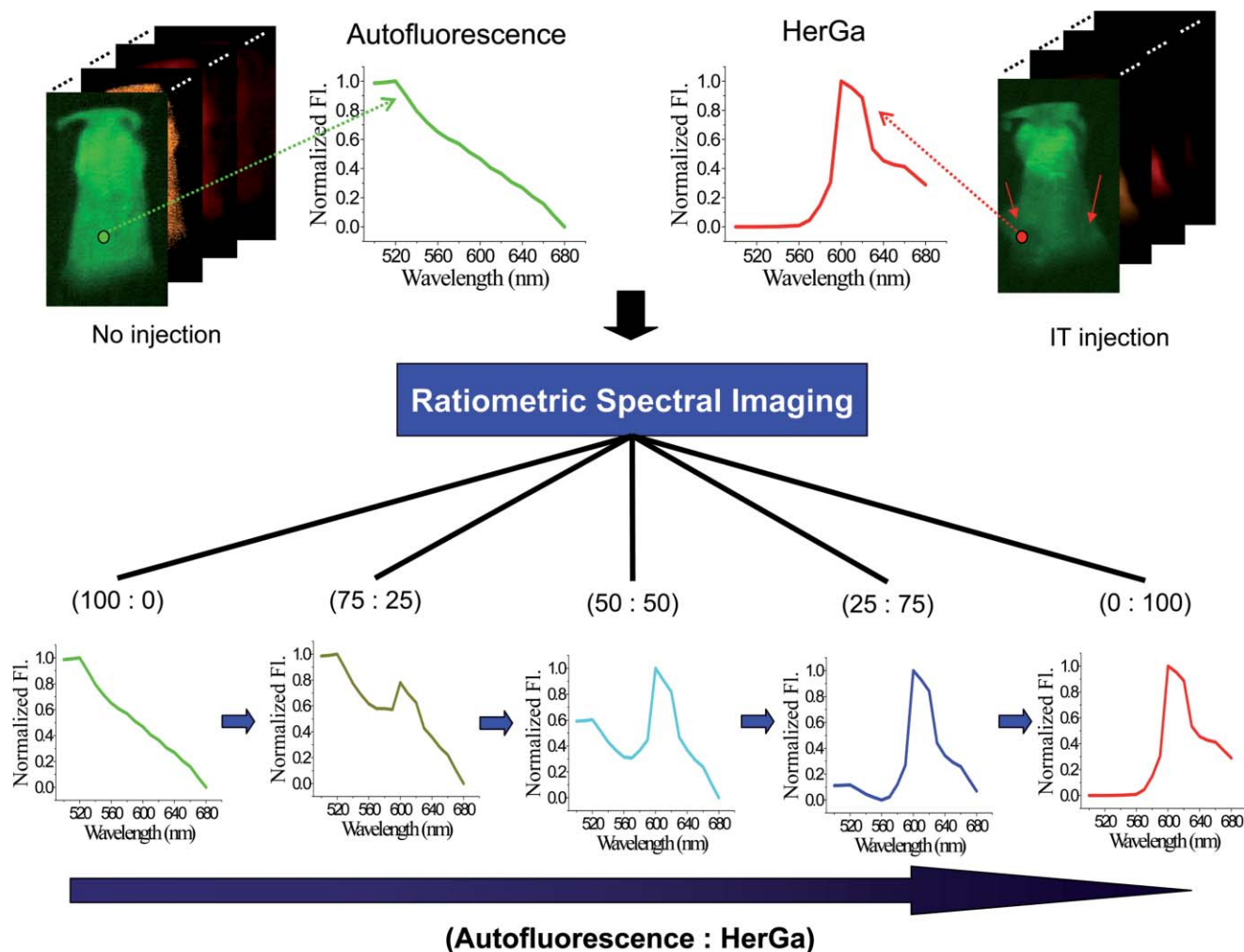
Fig. 1 Construction of composite spectra with varying ratios of spectra of autofluorescence and HerGa fluorescence: the pure spectral signatures of autofluorescence and HerGa fluorescence were obtained from the image cube before (upper-left) and after i.t. injection (upper-right). The ratiometric spectral imaging program generates the reference spectral signatures shown in the lower images with the pure spectral signatures.

We present here a novel *in vivo* ratiometric spectral imaging and analysis method that allows us to both monitor the specific accumulation of a novel chemotherapy molecule into breast tumors quantitatively and fast detect/delineate the tumors by the drug molecule. HerGa was chosen for these investigations because in addition to its chemotherapeutic effect for HER2+ breast tumor elimination, it is also an excellent fluorophore due to its intense fluorescence emission.[5] In the work described here, HerGa distribution over the nude mouse after its i.v. injection was monitored by using both the typical spectral imaging and analysis method and the ratiometric spectral imaging and analysis at different points in time, and then the outcomes were compared. In addition, we tested whether the ratiometric spectral imaging and analysis using HerGa can allow detection and delineation of the breast tumors. In the ratiometric spectral imaging and analysis, five reference spectral signatures were constructed by composite spectra with varying ratios of pure spectral signatures of autofluorescence and HerGa fluorescence using a program we developed. For spectral classification, a sum of area difference measure algorithm based on Euclidean distance calculation was utilized.[10]

2 Methods and Materials

2.1 *Materials*

HerPBK10 protein for tumor targeting and internalization was produced in *Escherichia coli* as a histidine-tagged fusion protein as described previously.[11] Gallium-metallated sulfonated corrole (S2Ga) was synthesized and combined with HerPBK10 at a molar ratio of 30:1 (based on the binding ratio of corrole to HerPBK10 that we typically observe) and any free S2Ga removed by ultrafiltration, as previously described.[4] The resulting HerGa complex was suspended in the phosphate-buffered saline for i.v. administration (46 nmoles) in female nude mice bearing HER2+ bilateral flank tumors (MDA-MB-435 tumors at $>300 \text{ mm}^3$).[5]

2.2 *Experimental Setup*

For examination of the specific accumulation of HerGa into tumor tissues, we utilized the spectral imaging mode in our multimode optical imaging system as described elsewhere.[12] For the excitation of HerGa, femtosecond (fs) pulsed laser light tuned

to 424 nm at a repetition rate of 80 MHz, was generated by the second harmonic of a fs pulsed laser at 848 nm (Mai-Tai Ti-Sapphire laser, Spectra-Physics). Also, we utilized an acousto-optic tunable filter (AOTF) (ChromoDynamics, Inc.) connected with a cooled CCD camera (PIXIS 400, Princeton Instruments) to perform sequential spectral selection of emission fluorescence from the specimen, with a 500 nm long-pass filter placed before the AOTF to reject the excitation light.

2.3 Construction of Reference Spectral Signatures for Ratiometric Spectral Imaging and Analysis

For the ratiometric spectral imaging and analysis, we constructed reference spectral signatures with varying ratios of pure spectral signatures of autofluorescence and HerGa fluorescence, respectively. In order to construct the pure spectral signatures, 10 sequential images were recorded within the spectral range of 500 to 680 nm with a step size of 20 nm and a bandwidth of 10 nm before and after the HerGa intratumoral (i.t.) injection. Then, spectral signatures of the autofluorescence and HerGa fluorescence were generated from the sequential images of a mouse using our custom-developed software.[13] We used two mice to construct reference spectral signatures, and selected a relatively large area for determining the spectral signatures of tissue autofluorescence and HerGa fluorescence (Fig. 1). While the spectral signature of autofluorescence (A) has a peak around 520 nm and decreases as the wavelength increases, the spectral signature of HerGa (H) has a peak around 620 nm, as shown in Fig. 1.

In realistic *in vivo* situations, the fluorescence from a nude mouse after i.v. injection of HerGa can be represented by the linear superposition of the two pure spectral signatures (A and H) as:

$$S = a_1 \times A + a_2 \times H,$$

where S is the composite spectral signature, A and H are the spectral signatures of autofluorescence and HerGa fluorescence respectively, and a_n is the relative contribution of the signals. Using the pure spectral signatures, we constructed five spectral signatures with 100:0, 75:25, 50:50, 25:75, and 0:100 ratios of A and H for spectral classification. The ratio indicates a relative HerGa contribution to autofluorescence. While the 100:0 ratio represents pure autofluorescence, the 0:100 ratio represents a high overall contribution of HerGa to the detected fluorescence. In contrast, the 75:25, 50:50, and 25:75 ratios represent the transition between the pure autofluorescence and the large amount of HerGa accumulation, respectively (Fig. 1). Thus, this approach can provide a relatively accurate quantitative estimate of the relative contribution of two sets of contributions (autofluorescence and HerGa fluorescence) and their variation in space and time *in vivo*.

2.4 Spectral Classification

For spectral classification, we utilized a sum of area difference measure based on Euclidean distance calculation, which we developed as a plug-in program for Image *J*.[13] In this classification, similarity values between the constructed reference spectral signatures and the spectral signature on each pixel of the image were calculated using the sum of area difference
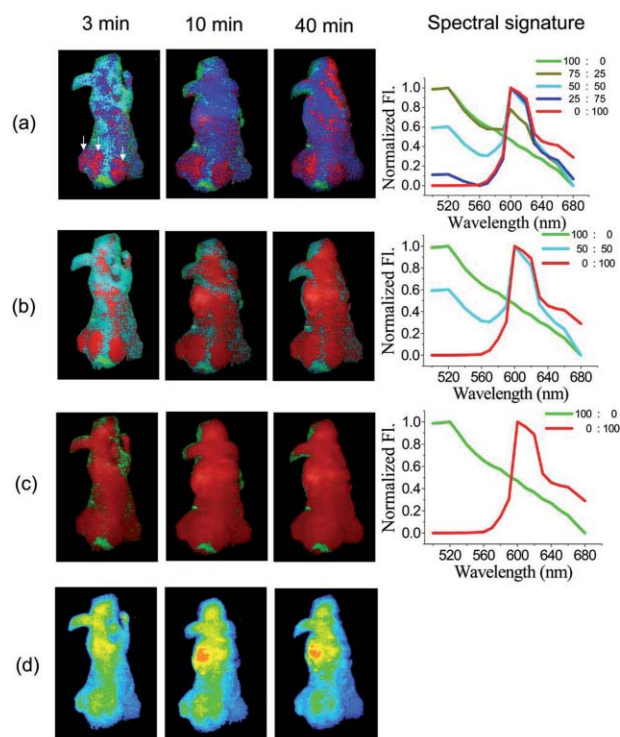

Fig. 2 Quantitative examination of HerGa accumulation into a mouse at different time points using ratiometric and standard spectral imaging and analysis: (a) ratiometric spectral classification using five reference spectral signatures (right, top), (b) ratiometric spectral classification using three reference spectral signatures (right middle), (c) standard spectral classification (two reference signatures, right bottom), (d) fluorescence intensity images. Arrows indicate tumor regions.

measure algorithm, and then each pixel was assigned to the specified spectral class. Finally, a pseudo-color display for each class was created for a classified image.

3 Results

3.1 HerGa Tumor Preferential Accumulation and Tumor Detection Capacity In Vivo

To monitor tumor-preferential accumulation and detection of HerGa after i.v. administration, we acquired consecutive images of the mouse within spectral ranges from 500 to 680 nm with a step size of 20 nm at different time points (3, 10, and 40 min after injection) using the system described earlier (total image acquisition time: 50 s). Then, the images were analyzed using ratiometric spectral imaging and analysis with three to five reference spectral signatures. In addition, the images were classified using a more traditional spectral analysis method, for comparison. Figure 2 shows the spectral classification images, the reference spectral signatures, and fluorescence intensity images obtained through three different methods at the time points mentioned earlier. In the spectral signatures, the ratios represent the relative intensity of autofluorescence and HerGa fluorescence. While the green pseudo-color (100:0 ratio) represents pure autofluoresence (A.F), the fluorescence spectral signature of highly concentrated HerGa in the mouse is represented by a red pseudo-color. The spectral signatures displayed with a deep

yellow, cyan, and blue colors show different ratios of relative contribution of HerGa to autofluorescence, respectively.

In the spectral classification images shown in Fig. 2(a), tumor regions (red pseudo-color) are clearly distinguished from the nontumor regions due to preferential accumulation of HerGa into the tumors compared to other regions at all time points compared to fluorescence intensity images. This result shows that the ratiometric spectral imaging and analysis with five reference spectral signatures allows the determination of the preferential tumor accumulation of HerGa, as well as discrimination between tumor and nontumor regions, quantitatively. Figure 2(b) shows that the tumor regions are properly distinguished from nontumor regions at 3 min. After 3 min, while the regions classified by the cyan pseudo-color (A.F: 50 and HerGa: 50) continue to shrink, the regions classified by the red pseudo-color (A.F: 0 and HerGa: 100) are expanded over the mouse. After 40 min, nearly the entire regions of the mouse are classified by the red pseudo-color (A.F: 0 and HerGa: 100). In contrast, the spectral classification images obtained using a standard spectral analysis method [Fig. 2(c)] show that the regions classified as HerGa are considerably distributed over the mouse at 3 min. Thus, the tumor regions are not discriminated from the nontumor regions due to HerGa accumulation. Furthermore, nearly the entire mouse is classified by the red pseudo-color (HerGa) after 3 min. Finally, as shown in the fluorescence intensity image [Fig. 2(d)], we could observe the changes of HerGa distribution across the mouse at the indicated time-points. In Fig. 2, HerGa preferential accumulation in the tumor was observed at the earlier time points whereas after 10 min, we also observe HerGa accumulation around the liver and heart regions. However, at this time, the fluorescence intensity imaging produces less clear discrimination between tumors and nontumor regions compared to the ratiometric spectral imaging and analysis. Therefore, these results indicate that ratiometric spectral imaging and analysis provides better quantification in monitoring HerGa accumulation into tumors than the standard spectral imaging analysis and fluorescence intensity imaging methods, and support the feasibility of using ratiometric spectral imaging and analysis for tumor detection and tumor accumulation of HerGa.

3.2 Quantitative Examination of HerGa Accumulation in Tumors From Excised Tissue

The *in vivo* results shown previously indicate that the ratiometric spectral imaging and analysis can provide better representation for monitoring HerGa accumulation into tumors and is likely to be useful for tumor detection. Here, we used ratiometric spectral imaging and analysis of tumors that were harvested from mice after tumor-accumulation of HerGa. In our previous studies, we have shown that the preferential accumulation of HerGa in tumors could be observed using fluorescence intensity imaging after the tumors were extracted from the mouse at 1 day after i.v. HerGa administration.[5] Here, tumors were extracted from the mouse at the 4th day after i.v. administration of HerGa in order to assess the extent of tumor retention and accumulation using ratiometric spectral imaging and analysis. Figure 3 shows the spectral classification images and the fluorescence intensity image obtained by each suggested method. While the fluorescence intensity image displays fluorescence (HerGa + autofluorescence) from tumors [Fig. 3(d)], the
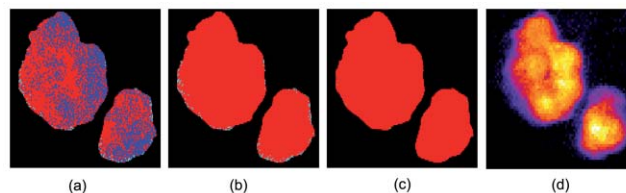

Fig. 3 The spectral classified images and fluorescence intensity image for quantitative examination of HerGa accumulation in tumors *ex vivo* obtained by using (a) ratiometric spectral classification using five reference spectral signatures, (b) ratiometric spectral classification using three reference spectral signatures, (c) standard spectral classification, (d) fluorescence intensity imaging (classification spectra were the same as in Fig. 2).

spectral classification images display the classification between HerGa and autofluorescence. In the spectral classification images, most of the tumor regions are classified as HerGa fluorescence, thus verifying that the fluorescence from tumor regions is specifically emitted from HerGa. Particularly, the spectral classification image obtained by the ratiometric spectral imaging and analysis with five reference spectral signatures [Fig. 3(a)] only displays red and blue pseudo colored regions, which represent the relative ratio of HerGa fluorescence and autofluorescence, 100:0 and 75:25, respectively. However, the other spectral images [Fig. 3(a) and 3(b)] do not. These findings suggest that the ratiometric spectral imaging and analysis can provide a more quantitative discrimination of HerGa accumulation in extracted tumors than standard spectral imaging and analysis. Altogether, we now verify that HerGa is still retained in the tumors even 4 days after HerGa administration, and that this tumor accumulation can be quantified using the ratiometric spectral imaging and analysis.

4 Discussion and Conclusions

In our previous study,[3] we identified limitations of our fluorescence imaging method, which may be considered typical for many presently used fluorophores. In particular, the 424 nm wavelength of light used for the excitation of HerGa *in vivo* produces significant autofluorescence, and its penetration depth through the tissues is shallow ($\sim$ millimeter), thus resulting in relatively low contrast in the determination of the preferential tumor-accumulation of HerGa. As shown in Fig. 2(d), we can observe the changes of HerGa accumulation in the tumor and liver regions at the indicated time-points. However, the image contrast in the determination of the preferential tumor-accumulation of HerGa also seems to be relatively low. At this point, it is important to mention that the detected fluorescence reflects the sum of autofluorescence, fluorescence from the skin, and fluorescence from tumors although the skin fluorescence comprises a large portion of these. However, we believe that the HerGa fluorescence from the tumors can still be detectable for the following reasons. First, HerGa accumulation occurred in a subcutaneous tumor in which typical skin thickness is approximately 400 μm.[14] Second, the wavelength of fluorescence emitted from HerGa is around 620 nm while excitation occurs at 424 nm. Given these parameters, HerGa fluorescence is more detectable *in vivo* than other fluorophores with blue excitation but exhibiting green emission.[15] Indeed, we have verified this

after i.t. injection of HerGa (data is not shown).[16] Moreover, our previous studies show, using fluorescence intensity imaging, that HerGa is clearly accumulated in tumors.[5]

In this work, we show that ratiometric spectral imaging and analysis is useful for monitoring the preferential accumulation of HerGa into HER2+ breast tumors at sequential time points, and is more quantitative than both standard spectral imaging and fluorescence intensity imaging. In the ratiometric spectral classification images [Fig. 2(a) and 2(b)], we could clearly distinguish between tumor and nontumor regions by preferential tumor accumulation of HerGa at the earlier time points. The results show that HerGa accumulated into tumors earlier and more intensely than into other regions after i.v. injection. This is likely due to a combination of HerGa binding to HER2+ cells and enhanced tumor vascularization.[17] However, in the standard spectral classification image [Fig. 2(c)], the discrimination between tumor and nontumor regions due to HerGa accumulation was not possible at the early time points. Moreover, in the examination of HerGa accumulation in tumors *ex vivo,* the ratiometric spectral imaging and analysis also provides more quantitative information regarding the HerGa tumor accumulation than other methods, as shown in our *in vivo* study. Therefore, we conclude that ratiometric spectral imaging and analysis enables the monitoring of the accumulation of HerGa more quantitatively than the typical spectral imaging and analysis methods, and has the potential to detect and delineate the tumor locations in the earlier time points *in vivo*. In addition, the quantitative capacity of this method is increased as the number of reference spectral signatures with varying ratios of A and H is increased.

In this study, we considered the earlier time-points since the accumulation of HerGa in other tissues such as skin, becomes higher at longer time-points after i.v. HerGa injection than the indicated time-points. Eventually, the spectral signature of fluorescence from skin becomes similar to the spectral signature with the ratio of autofluorescence: HerGa, 0:100, and then the ratiometric spectral imaging and analysis, also does not allow us to monitor any quantitative accumulation of HerGa in tissues and discriminate between tumors and other regions as the standard spectral imaging and analysis. In addition, the vascularization (angiogenesis) around tumors is much richer than in other tissues such as skin and surrounding muscles. This may allow for more HerGa accumulation in the tumor at the earlier time-points and provides better chances to detect the tumor regions using the ratiometric spectral imaging and analysis method at the earlier time-points. Much longer time-points, when HerGa is washed out from the skin, may also be well suited for tumor detection using this ratiometric spectral imaging and anaysis.

In conclusion, we have demonstrated and validated the potential of a simple *in vivo* ratiometric spectral imaging and analysis method for dynamic monitoring of HerGa accumulation into tumor regions and for tumor detection. The results suggest that this method can provide better quantitative information than standard ones, and better specificity than standard fluorescence intensity imaging. In addition, this ratiometric spectral imaging and analysis may be applicable to most other chemotherapy and photodynamic therapy molecules.[8, 18] Particularly, it may be very useful for quantitative monitoring of the distribution of drug molecules labeled with quantum dots, where blue light excitation and ratiometric spectral imaging and analysis, applied together, are less sensitive to autofluorescence and excitation beam spectral profiles. In the clinical setting, fast and accurate determination[19] of the location of tumors is crucial for successful outcomes; the ratiometric spectral imaging and analysis with HerGa as shown here may thus be useful for speeding up tumor detection and for topological outlining for surgical intervention. Finally, translating this method into the clinic for cancer management could pave the way for fast, accurate prognosis and therapy, by better spatiotemporal coupling of detection and intervention.

References

1. C. Lohrisch and M. Piccart, "An overview of HER2," *Semin. Oncol.* **28**(6), 3–11 (2001).
2. M. Colombo, F. Corsi, D. Foschi, E. Mazzantini, S. Mazzucchelli, C. Morasso, E. Occhipinti, L. Polito, D. Prosperi, S. Ronchi, and P. Verderio, "HER2 targeting as a two-sided strategy for breast cancer diagnosis and treatment: Outlook and recent implications in nanomedical approaches," *Pharmacol. Res.* **62**(2), 150–165 (2010).
3. J. Y. Ljubimova, M. Fujita, N. M. Khazenzon, B. S. Lee, S. Wachsmann-Hogiu, D. L. Farkas, K. L. Black, and E. Holler, "Nanoconjugate based on polymalic acid for tumor targeting," *Chem. Biol. Interact.* **171**(2), 195–203 (2008).
4. H. Agadjanian, J. J. Weaver, A. Mahammed, A. Rentsendorj, S. Bass, J. Kim, I. J. Dmochowski, R. Margalit, H. B. Gray, Z. Gross, and L. K. Medina-Kauwe, "Specific delivery of corroles to cells via noncovalent conjugates with viral proteins," *Pharm. Res.* **23**(2), 367–377 (2006).
5. H. Agadjanian, J. Ma, A. Rentsendorj, V. Valluripalli, J. Y. Hwang, A. Mahammed, D. L. Farkas, H. B. Gray, Z. Gross, and L. K. Medina-Kauwe, "Tumor detection and elimination by a targeted gallium corrole," *Proc. Natl. Acad. Sci. U.S.A.* **106**(15), 6105–6110 (2009).
6. R. D. Shonat, E. S. Wachman, W. Niu, A. P. Koretsky, and D. L. Farkas, "Near-simultaneous hemoglobin saturation and oxygen tension maps in the mouse cortex during amphetamine stimulation," *Adv. Exp. Med. Biol.* **454**, 149–158 (1998).
7. S. Tomatis, M. Carrara, A. Bono, C. Bartoli, M. Lualdi, G. Tragni, A. Colombo, and R. Marchesini, "Automated melanoma detection with a novel multispectral imaging system: results of a prospective study," *Phys. Med. Biol.* **50**(8), 1675–1687 (2005).
8. X. Gao, Y. Cui, R. M. Levenson, L. W. Chung, and S. Nie, "*In vivo* cancer targeting and imaging with semiconductor quantum dots," *Nat. Biotechnol.* **22**(8), 969–976 (2004).
9. J. G. Fujimoto and D. L. Farkas, *Biomedical Optical Imaging*, Oxford University Press, Oxford (2009).
10. V. K. Ramanujan, E. Biener-Ramanujan, K. Armmer, V. E. Centonze, and B. A. Herman, "Spectral kinetics ratiometry: a simple approach for real-time monitoring of fluorophore distributions in living cells," *Cytometry A* **69**(8), 912–919 (2006).
11. L. K. Medina-Kauwe, M. Maguire, N. Kasahara, and L. Kedes, "Nonviral gene delivery to human breast cancer cells by targeted Ad5 penton proteins," *Gene Ther.* **8**, 1753–1761 (2001).
12. J. Y. Hwang, C. Moffatt-Blue, O. Equils, M. Fujita, J. Jeong, N. M. Khazenzon, E. Lindsley, J. Ljubimova, A. G. Nowatzyk, D. L. Farkas, and S. Wachsmann-Hogiu, "Multimode Optical Imaging of Small Animals: Development and Applications," *Proc SPIE* **6441**, 644105 (2007).

13. A. Chung, S. Karlan, E. Lindsley, S. Wachsmann-Hogiu, and D. L. Farkas, "*In vivo* cytometry: a spectrum of possibilities," *Cytometry A* **69**(3), 142–146 (2006).
14. J. Fuchs, N. Groth, and T. Herrling, "Spectral-spatial electron paramagnetic resonance imaging (EPRI) in skin biopsies at 9.5 GHz," *Methods Mol. Biol.* **196**, 221–226 (2002).
15. R. M. Hoffman, "*In vivo* imaging of metastatic cancer with fluorescent proteins," *Cell Death Differ.* **9**(8), 786–789 (2002).
16. J. Y. Hwang, H. Agadjanian, L. K. Medina-Kauwe, Z. Gross, H. B. Gray, K. Sorasaenee, and D. L. Farkas, "Large field of view scanning fluorescence lifetime imaging system for multimode optical imaging of small animals," *Proc SPIE* **6859**, 68590G (2008).

17. D. Lyden, K. Hattori, S. Dias, C. Costa, P. Blaikie, L. Butros, A. Chadburn, B. Heissig, W. Marks, L. Witte, Y. Wu, D. Hicklin, Z. Zhu, N. R. Hackett, R. G. Crystal, M. A. Moore, K. A. Hajjar, K. Manova, R. Benezra, and S. Rafii, "Impaired recruitment of bone-marrow-derived endothelial and hematopoietic precursor cells blocks tumor angiogenesis and growth," *Nat. Med.* **7**(11), 1194–1201 (2001).
18. G. Palumbo, "Photodynamic therapy and cancer: a brief sightseeing tour," *Expert Opin. Drug Deliv.* **4**(2), 131–148 (2007).
19. P. K. Frykman, E. H. Lindsley, M. Gaon, and D. L. Farkas, "Spectral imaging for precise surgical intervention in Hirschsprung's disease," *J. Biophotonics* **1**, 97–103 (2008).